

# Land Systems Response to Water Footprint in the Wooded Savannah of Western Nigeria

Mayowa Fasona<sup>1</sup>, Mark Tadross<sup>2</sup>, Babatunde Abiodun<sup>2</sup>, Ademola Omojola<sup>1</sup>  
<sup>1</sup>*Department of Geography, University of Lagos, Lagos, Nigeria;* <sup>2</sup>*Climate Systems Analysis Group, University of Cape Town, Cape Town, South Africa*

\*Corresponding author's e-mail: [mfasona@unilag.edu.ng](mailto:mfasona@unilag.edu.ng) / [mfasona@yahoo.com](mailto:mfasona@yahoo.com)

## Abstract

Erratic space and time distribution of rainfall coupled with increase in temperature means less water. The water footprint, therefore, will be critical for future development in dry and semi-dry areas where survival for large population depends on rainfed agriculture and the natural resource stock. This study investigates the linkage between water footprint and land system changes. Present and projected future rainfall and temperature data were integrated with local eco-geographical factors and subjected to principal component analysis (PCA) to decipher the present and future pattern of water footprint. These integrated dataset was also analyzed to build change drivers which were applied to satellite image derived land-cover maps to project future land-cover pattern under both present and future climate scenario using Idrisi's dynamic CA\_Markov land change model. The results suggest the emerging and future spatial pattern of ecosystems, agricultural land-use and agrarian settlements will largely follow the water footprint. Under future climate scenario (2046-2065) galleria forest - a signature of the drier savannah - is projected to dominate much of the presently forested landscapes and this will correspondingly shift the water footprint and thus alter the spatial and temporal pattern of agricultural land-use and settlement locations.

## Introduction

The relationship between climate and terrestrial ecosystems is characterized by a two-way feedback. Change in land-cover has strong effect on the climate system and change in the system also has the potential to alter the pattern of land-cover across space and time. While a change in land-cover may strongly influence the pattern of rainfall, evapotranspiration and temperature, ecosystems changes on a broader scale such as transition of woodlands or deciduous forests to grasslands and pastures, or grassland to bare surface may result from a change in the climate system. While much is now known about the possible impacts of ecosystem changes on the climate system (Wang and Eltahir, 2000; Taylor *et al.*, 2002; Afiesimama *et al.*, 2006; Pielke *et al.*, 2007; Abiodun *et al.*, 2008; MacKellar *et al.*, 2009), the potential of the climate system to influence patterns of ecosystem changes across space and time has not received considerable attention. The latter part needs to be better understood in the context of today's requirements for place-based and context-specific adaptation measures.

Long-term climate patterns may well exert some control over vegetation type and canopy structure. In particular, rainfall and temperature changes strongly influence the presence and distribution of specific ecosystems, plant species and patterns of natural resource systems (Solomon *et al.*, 2007; German Advisory Council on Climate Change, 2008). These changes could also trigger the spatial reorganization of both agrarian land-use and settlement systems and access to livelihoods in poor societies that rely on rain-fed agriculture and natural resource stock. Long term rainfall signals have already become more erratic in space and time distribution in the arid and semi-arid regions of West Africa, including the Nigerian savannah (Nicholson, 2000; Afiesimama *et al.*, 2006; Abiodun *et al.*, 2008), yet a large population depends on small holder, rainfed agricultural systems. Thus, the water footprint may become more critical in defining the future pattern of settlements and trajectory of agrarian land-uses.

According to Hewitson and Crane, 2006, a degree of local forcing that varies by region and season often complement synoptic-scale forcing to influence the local climate. Local perturbations including terrain, land-cover, and land-water boundary often exert strong influence on the local climate and create water footprint that support the natural resource capita on which livelihoods of rural population thrive. Rainfall is a critical limiting factor of human activity in the savannah and prolonged change in its quantity and regime is an index of climatic variability and change. Monsoonal wind and the mesoscale convective process (MCS) are the dominant rain producing forces over the region. The MCS relies on the complexity in terrain and land-cover to propagate and accounts for over 75% of rainfall received in the West Africa savannah (Omosho and Abiodun, 2007). The relatively coarse resolution of global and regional climate models often mask large differentials in local forcing and local scale circulation and perturbation which are critical for local water footprint.

The focus of this study is to investigate local climate induced water footprint and its potential to define the pattern and trajectory of ecosystems change, agricultural land-use and settlement systems across

space and time. Understanding this relationship could be critical for designing climate change mitigation and adaptation measures at local levels.

## Material and Methods

### Regional setting

The study area is roughly defined by Latitudes  $8^{\circ}$  to  $9^{\circ}15'$  North and Longitudes  $3^{\circ}50'$  to  $5^{\circ}50'$  East. It covers about  $40,000\text{km}^2$  in western Nigeria, extending from the border with Benin Republic in the west to the Niger floodplains in central Nigeria covering parts of Oyo, Kwara, Kogi, Niger, Ekiti and Osun States (Fig.1).

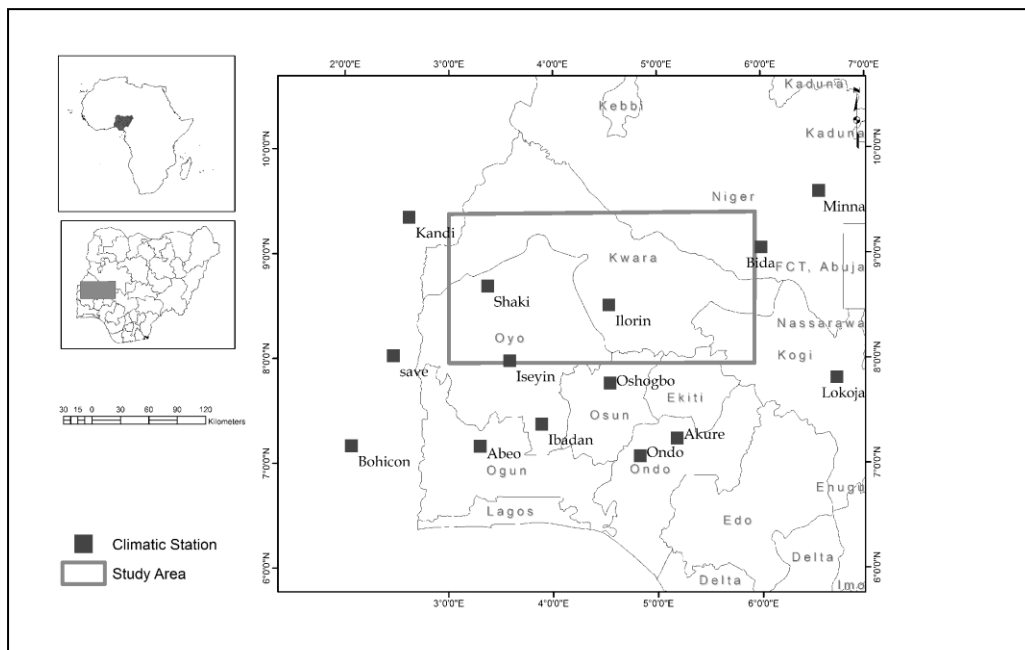


**Fig. 1: Study area and observation stations**

The study area is characterized by the wooded savannah vegetation and lies in the transitional zone between the southern rainforest and the northern grassland savannah. Average elevation is about 300 m but with outcrops rising above 500 m in the eastern axis. Vegetation consists of mixture of trees and grasses, as well as moist peri-forest mixed with savannah of anthropic degradation and patchy landscape (Hoffmann and Jackson, 2000; Bucini and Lambin, 2002). Generally, the area is characterized by a sub-humid Koppen's *Aw* climate (Kottek *et al.*, 2006). Annual rainfall is between 900 mm and 1300 mm and the mean maximum temperature range between  $28^{\circ}\text{C}$  and  $36^{\circ}\text{C}$  with peak

temperature occurring at February and March. The southern part shares the bimodal rainfall pattern of the southern rainforest belt with peaks in mid June to July and September. The highest monthly rainfall occurs in September as opposed to July for the rainforest belt.

Population density is high and poverty-environment linkage is very strong. The study area is important for root, tuber and cereal cultivation. Intense land-use pressure has increased the frequency of savannah fire, forest conversion to agricultural land, and incursions into marginal lands. Uncontrolled harvesting of trees for fuel-wood and charcoal are important livelihood activities (Akinbami *et al.* 2003). Due to its large pasture undergrowth, the study area has in recent years become important for extensive grazing for migrating pastoralists. This has increased the frequency of land resource conflict (Fasona and Omojola, 2005; Obioha, 2008; Adisa and Adekunle, 2010).

### **Data utilized**

Satellite imagery and terrain data

Six georeferenced and orthorectified Landsat scenes (p190r054 of 15 November 1986, p191r054 of 27 December 1990, p190r054 of 13 November 2000, p191r054 of 06 February 2000, p190r054 of 14 November 2006, and p191r054 of 18 November 2005) were accessed from Landsat Geocover datasets ([www.landcover.org/data/](http://www.landcover.org/data/)). Terrain derivatives, including slope, aspect, contours, and spot heights, were generated from Shuttle Radar Topography Mission (SRTM) three-arc-second digital elevation model data . Present and future climate

Data for historical daily rainfall and maximum temperature (*T<sub>max</sub>*) for 12 climatic stations around the study area and adjacent stations in Benin Republic were acquired from the archives of the Nigerian Meteorological Agency (NIMET) and the portal of the Climate Systems Analysis Group (CSAG), University of Cape Town ([www.csag.uct.ac.za](http://www.csag.uct.ac.za)) respectively. Statistical downscaling of the data was carried out by CSAG. The statistical downscaling technique employed matching of GCM data with self organized map (SOM) characterization of atmospheric states and was forced by an SRES A2 emissions scenario (Hewitson and Crane 2006). The driving GCMs employed were adopted from the

Coupled Model Intercomparison Project Phase Three (CMIP3) archive (<http://www.pcmdi.llnl.gov/projects/cmip/Table.php>), which makes statistical downscaling possible only for the non-seamless periods of 2046-2065 (near future) and 2081-2100 (far future). The statistical downscaling reproduced the observational data and produced both near-future and far-future projections for 10 GCMs and NCEP reanalysis. A comparability study of GCMs carried out by Cook and Vizy (2006) suggested that the Japanese MRI CGCM 2.3.2 model provides the most reliable simulation of the twenty-first century climate over West Africa. The downscaled data from MRI CGCM was adopted for input into the PCA and land modeling analysis.

Other datasets used include the 1:650,000 soil data produced by the Soils Survey Division of the Nigerian Ministry of Agriculture and Natural Resources and the 1:250,000 Vegetation and Land use data produced in 1995/96 by the Forestry Resources Mapping, Evaluation and Coordination Unit (FORMECU) of the same Ministry. Population data were obtained from the archive of the Nigerian National Bureau of Statistics.

## **Procedure**

### *Framework*

The Landsat images were subjected to band compositing using Idrisi® Taiga software ([www.clarklabs.org](http://www.clarklabs.org)). A land-cover classification schema derived from the USGS land-use/land-cover (LULC) schema (Anderson *et al.* 1976) was used. The maximum likelihood (MAXLIKE) classification algorithm was adopted because the training sites were well defined with large sample sizes. Refinement and modification of the classification outputs led to a reduction of the initial 25 categories to a final 13 categories. The output was subjected to a Markovian probability estimator to generate conditional probabilities for the prediction of future land-cover change. Change drivers, including present and future rainfall,  $T_{max}$ , soil potential for agriculture, protected area, population density, contour, slope, and aspect were used as factor inputs to build composite change suitability maps using multi-criteria analysis. The combination of the suitability maps and land-cover-derived

Markov conditional probability maps were the input for the Cellular Automata-Markov (CA-Markov) model. The change drivers were also processed into gridded derivatives which were integrated into a common GIS database for collocation analysis. The output from the gridded derivatives was exported in ASCII text to statistical software and subjected to principal component analysis (PCA). The seasonal correlations and principal factors were generated and the result was imported back to GIS for spatial interpolation to derive PCA maps (Fig 2).

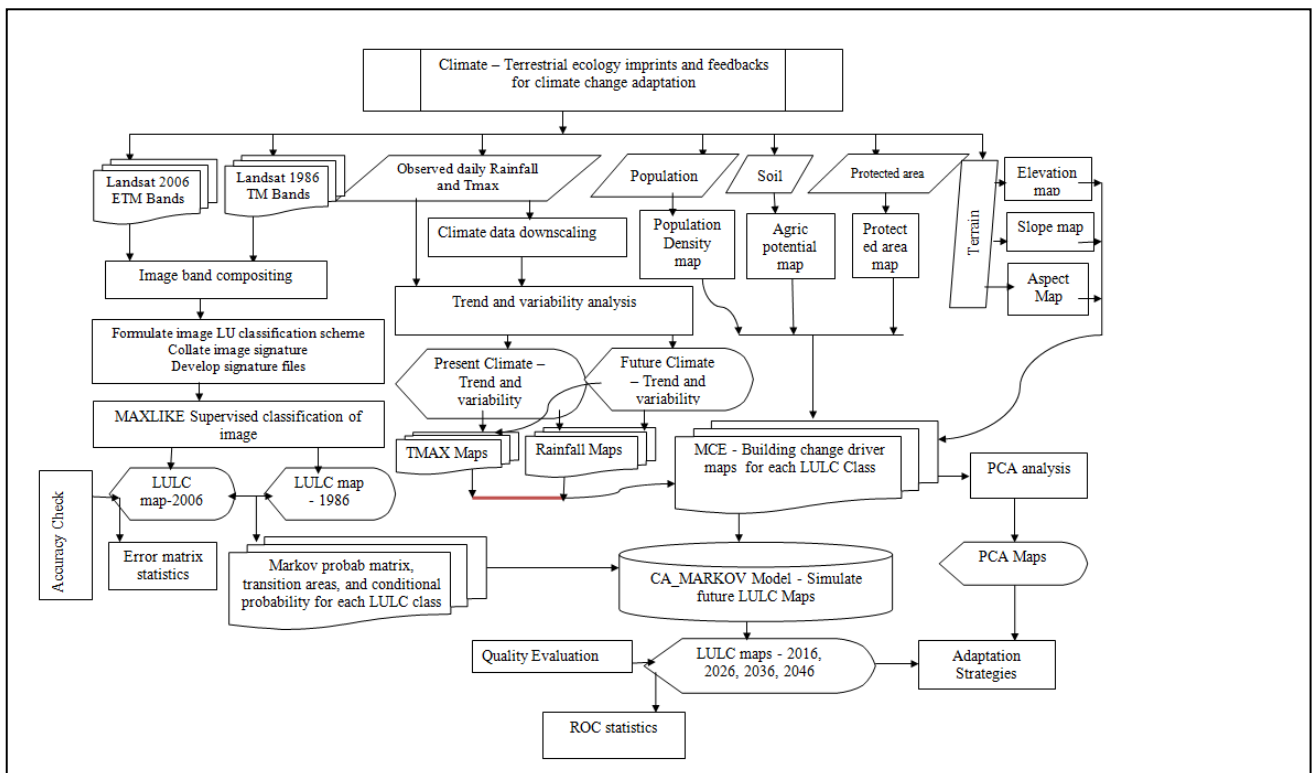


**Fig 2: Methodological Framework for the research**

Model description and experimental set-up for land change projection

*Deriving Markovian transition areas and conditional probability*

Land change models attempt to couple socio-ecological systems and thus require spatial explicitness. LULC change could be regarded as a stochastic process, with the different categories as the states of the chain (Weng 2002). Land-cover in the wooded savannah is highly heterogeneous, and the land-use system is complex; thus LULC change tends to be compatible with first order Markovian dependency.

The CA-Markov model exhibits spatial explicitness, allows the use of multiple categories, and can simulate the transition from one category to another.

(Eastman 2009). It acquires predictive power by combining Markov conditional probabilities and transition areas for each category with suitability maps for each category. CA-Markov deals with complications associated with competition in land-change among different pixels by implementing a multiple objective land allocation (MOLA) framework. The spatial explicitness property enables the model to predict both the quantity and location of each category using a suitability map for each transition that it extrapolates. At every time step, it determines the number of pixels that must undergo each transition, then selects the pixels according the largest suitability for the particular transition (Pontius and Malanson 2005; Eastman 2009).

CA-Markov accepts land-cover data from two time points (before and present) as inputs and generates outputs that include transition area files, a transition probability matrix, and a set of conditional probability maps, one for each land-cover category. The cellular automata (CA) component of the model guides the transition probabilities of one pixel to be a function of both the previous state and the state of the local neighborhood, i.e., neighboring pixels. It also helps to filter the suitability of land away from existing areas of that category during iteration and thus provides the model with some explanatory power. The net result is that land-cover changes develop as growth processes in areas of high suitability proximate to existing areas (Hall *et al.* 1995; Pontius and Schneider 2001; Pontius and Malanson 2005; Eastman 2009).

#### *Preparation of suitability maps*

The process of constructing the suitability maps involves the conversion, transformation and integration of several raster and vector data layers. The suitability maps were generated using the multi-criteria evaluation (MCE) module of Idrisi® Taiga. These suitability maps basically represent the integration of the driver maps. Each data layer was standardized and converted into the integer format accepted by the MCE module. The driver maps that defined the criteria in the MCE are divided into factors and constraints. Factors are generally continuous variables (including slope, aspect, elevation, rainfall, temperature) and indicate the relative suitability of certain areas.

Table 1: Criteria for generating suitability maps in MCE

Code	LULC Class	Factors and score	Constraints
1	Urban	Elevation (0.6)+ slope (0.4)	distance to water body and protected areas
2	Woodland	Mean annual rainfall (0.6)+ mean maximum temperature (0.4)	soil potential for agric
3	Forest	Mean annual rainfall (0.4)+ mean maximum temperature (0.4) + Elevation (0.2)	soil potential for agric
4	Shrub/grassland	Aspect (0.6)+ mean maximum temperature(0.4)	
5	Wetland	Aspect (0.4)+ Mean annual rainfall (0.6)	mean maximum temperature
6	Cultivation /commercial agric	Mean annual rainfall (0.6)+ mean maximum temperature (0.4)	soil potential for agric
7	Farmland/fallow/grazing area	Mean annual rainfall (0.6)+ mean maximum temperature (0.4)	distance to water body
8	Floodplain agric	Mean annual rainfall (1)	soil potential for agric
9	Water	Mean annual rainfall (1)	mean maximum temperature
10	Bare surface	mean maximum temperature (0.4)+Elevation (0.4)+ aspect (0.2)	distance to water body
11	Alluvial	Mean annual rainfall (1)	slope
12	Burnt surface	Mean maximum temperature (1)	distance to water body
13	Cloud /shadow	Mean annual rainfall (1)	

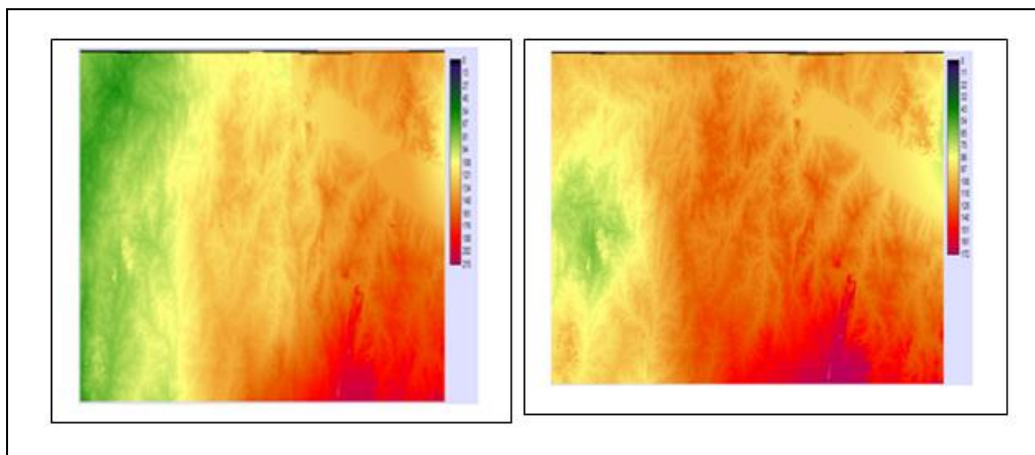


Fig 3: Suitability map for Class 3 (forest) under present (left) and future (right) climates

Each factor represents a fraction of the total factor that drive the land-cover category, the total weight point for all factors for that category is therefore equal 1. The higher the factor weights, the greater their influence on the final suitability maps. Constraints are Boolean (0 or 1) and include criteria such as distance to water bodies, soil potential for agriculture and protected areas. Constraints serve to exclude certain areas from consideration in the competition for land-change for that category. Only 8

of the initial 13 defined criteria were used to generate the final suitability maps for the 13 LULC categories (Table 1 and Fig. 3); the others were eliminated for collinearity.

### Model simulation

Each model run uses the suitability map collection with the basis land-cover map (image-derived 2006 map), Markov transition areas file, and conditional probability matrices to simulate future land-cover, placing simulated change in cells that have the largest suitability values. If the suitability map was perfect, the order of the suitability values would match the order in which humans change the landscape, with the largest suitability values being changed first (Hall *et al.* 1995; Pontius and Schneider 2001). The model was run for 4 scenarios: 2006 to 2016, with 10 iterations (1-year time-step); 2006 to 2026, with 20 iterations (1-year time-step); 2006 to 2036, with 15 iterations (2-year time-step) and 2006 to 2046, with 20 iterations (2-year time-step). To validate the simulated results, we used the 1986 and 2000 land-cover maps for initialization and then used the land-cover map of 2000 as the basis land-cover and perform an additional run (2000 to 2006) with 12 iterations (6-month time-step). For all model runs, the standard 5 x 5 contiguity filter was used.

Within each time step, each land-cover class was considered in turn as a host category. All other land-cover classes act as claimant classes and compete for land (only within the host class) using the MOLA procedure. The area requirements for each claimant class within each host were equal to the total established by the transition area file divided by the number of iterations. Whereas the demand for land by different land-cover categories determines the overall competitive capacity of each land-cover type, the location's suitability is a major determinant of the competitive capacity of each land-cover type at a specific location (Verburg, *et al.* 2007). We carried out two sets of simulations i.e. under both present and future climate scenarios using the present and future rainfall and maximum temperature as a driver input into the MCE suitability images.

## Results and discussion

### PCA of the water footprint

Eighteen (18) variables (15 for future climate) were generated, integrated and analyzed. The target is to identify the combination of factors (i.e. factors coupled into systems) that have impacts on the local climate. Tables 2 and 3 show the rotated (varimax with Kaiser Normalization) results of component matrix generated through correlation matrix for the present and future climates respectively.

Table 2: Extracted principal components for present climate

Variables	Component					
	1	2	3	4	5	6
Aspect	.129	-.116	.220	-.138	.621	-.287
Slope	-.075	.156	.236	.274	.014	-.534
Elevation	-.818	-.018	.292	.063	.059	.060
Population density	-.168	.234	-.062	.289	-.062	.312
Soil potential for agric	.099	.081	.320	.130	.119	.663
Distance to water	-.076	-.023	.111	.534	-.017	.154
Protected areas	.175	.215	-.292	.503	-.135	-.001
NDVI for 1986	-.210	-.001	.770	.156	-.059	-.026
NDVI for 2006	-.096	.156	.756	-.195	.018	.041
Average Tmax for 1986	.958	.033	-.045	.050	.028	.057
Average Tmax for 2006	.961	-.037	-.049	.087	-.007	.054
Average rainfall for 1986	.125	.931	.008	-.005	-.024	-.019
Average rainfall for 2006	-.650	.690	.069	-.045	.056	-.013
Disturbance index for 1986	-.162	-.063	-.030	.097	.760	.292
Disturbance index for 2006	.055	-.200	.126	.642	.215	-.117
Forested areas in 1986	.001	-.090	.465	-.176	-.660	-.019
Forested areas in 2006	-.121	-.058	.393	-.681	-.070	.136
Long-term mean rainfall	-.048	.915	.097	.007	-.080	.035

Table 3: Extracted principal components for future climate (2046-2065)

Variables	Component					
	1	2	3	4	5	6
Aspect	-0.035	-0.094	0.431	0.383	0.052	0.387
Slope	0.133	-0.150	-0.199	-0.208	-0.031	0.756
Elevation	0.823	-0.157	0.192	-0.197	-0.120	0.007
Population Density	0.151	-0.285	-0.286	-0.049	-0.197	-0.446
Soil potential for agriculture	-0.005	-0.085	0.010	0.172	-0.848	0.022
Distance to water	-0.029	-0.387	-0.016	-0.376	-0.317	-0.008
Protected area	-0.241	-0.406	-0.504	-0.085	0.108	-0.039
Disturbance index for 1986	0.100	-0.535	0.438	0.421	-0.152	-0.077
Disturbance index for 2006	-0.182	-0.523	0.217	-0.372	-0.110	0.173
Forest area in 1986	0.112	0.640	-0.086	-0.482	-0.267	0.058
Forest area in 2006	0.295	0.654	0.288	0.157	-0.243	0.005
Long term average rainfall	0.746	-0.025	-0.518	0.294	-0.035	0.108
Monthly average rainfall	0.746	-0.026	-0.518	0.294	-0.034	0.107
Long term average Tmax	-0.867	0.114	-0.292	0.207	-0.169	0.093
Mean monthly Tmax	-0.867	0.104	-0.283	0.209	-0.172	0.096

Six principal components explain 65.6% of the total variance between the extracted data for the present climate. The first principal component couples the climate-orographic complex and explains 20% of the total variance. It accounts for the coupled system between elevation, temperature and rainfall. Elevation is inversely related to temperature and directly related to rainfall. It also supports the assumption that mesoscale processes which relies on orographic forces controls the local climate. The second, third and fourth principal components show inter-correlations between the same set of variables i.e. rainfall, NDVI and forested areas respectively. Principal components five and six, though explain only 7% and 6% of the variance respectively, combine factors which include aspect, forested area, slope and soil potential for agriculture which are important for the ecological systems and use of the land.

For the future climate, 6 principal components accounted for 69% of the total variance. The coupled climate-orographic complex still remains the controlling system and accounts for about 24% of the total variance. The second principal component establishes inter-relationship between the forested areas in two different periods, and the third principal component establishes the direct positive feedback between rainfall and protected areas.

### **Spatial pattern of the water footprint**

The dominance of 'climate-terrain' complex on the local climate system is unassailable in both present and projected future climates. In both cases, elevation exerts positive influence on rainfall and negative influence on temperature. This pattern predominates from the southeast to northwest corridor and it is more pronounced in areas south of the city of Ilorin and around 'Oke-ogun' areas. The seasonal analyses suggest that this pattern predominates for present and future climates in all seasons except for June, July and August (JJA) when the system is reversed. Incidentally, the agricultural land-use around the southeast to northwest corridor is dominated by rainfed small-holder root, tuber and cereal cultivation which are well suited to the optimum rainfall and lower temperature that prevail

in this axis. On the other hand, onset of rains in the inland basins across the Niger is around May to June which coincides with the approach of the monsoon. Peak rainfall is received in August, the same time when ‘the little-dry season’ pervades the southeast to northwest corridor. These feedbacks also contrast the general notion of a regular rainfall gradient that decreases with latitude in the Nigerian savannah.

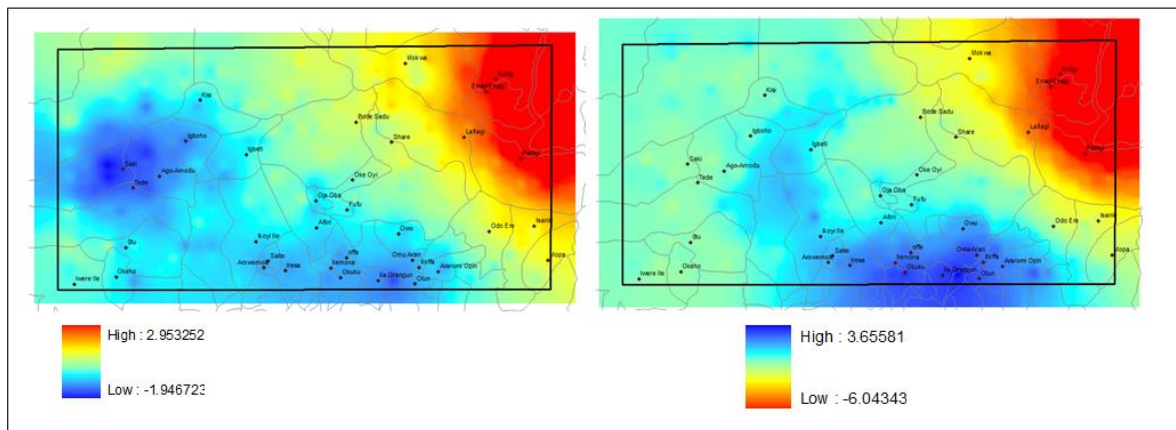


**Fig 4: The annual average: Rain and Tmax sensitivity to terrain (a) Present climate (-Elevation, -rain, +Tmax) (b) future climate (+Elevation, +rain, -Tmax)**

This spatial pattern is projected to continue in future climate (Fig. 4) but with diminishing influence. While the system is projected to become pronounced in the highland areas located at the edge of the rainforest zone in the southeast axis, its influence around the northwest corridor especially in ‘Okeogun’ areas will diminish.

### **Projected LULC change from 2006 to 2046**

Projected LULC from the present climate

The present climate for the wooded savannah is characterized by a maximum temperature increase on the order of approximately 0.06°C/month/decade, with the years 1998 to 2006 (except 1999) exhibiting continuously increasing maximum temperature anomalies. Rainfall increased marginally by approximately 0.6 mm/month/decade. Table 4 shows a comparison of the percent coverage of each land-cover category in 1986 and 2006 and their projected coverage for 2016 to 2046 under the present climate scenario.

Table 4: Percent coverage of current (1986 and 2006) and projected (2016 to 2046) LULC under present climate scenario

SN	LULC Class	Mapped		2016	2026	2036	2046
		1986	2006				
1	Urban	0.80	1.45	2.82	3.93	4.82	5.36
2	Woodland	19.70	32.11	20.68	26.93	23.09	22.62
3	Forest	13.48	15.63	18.36	15.12	15.06	14.68
4	Shrub/grassland	3.27	12.95	21.55	26.74	27.21	27.20
5	Wetland	5.27	4.14	2.55	1.64	1.89	1.50
6	cultivation/commercial agric	11.07	8.16	12.34	9.84	10.17	10.44
7	Farmland /fallow/grazing area	32.61	16.79	8.21	4.80	6.89	6.79
8	Floodplain agric	4.16	5.63	6.81	4.38	3.51	3.61
9	Water	0.55	0.70	1.23	1.67	2.07	2.45
10	Bare surface	2.61	1.23	1.01	1.33	1.53	1.59
11	Alluvial	0.04	0.03	0.02	0.01	0.02	0.01
12	Burnt surface/fire scar	5.84	0.15	0.67	0.49	0.46	0.52
13	Cloud /shadow	0.61	1.04	3.74	3.13	3.27	3.22

Footprints associated with discontinuous small-holder, rain-fed agriculture generally dominates the landscape in the wooded savannah of Nigeria. This is consistent with the findings of Tiwari *et al.* (2010) related to land-use dynamics in southern India. A comparison of the 1986 and 2006 LULC maps suggests significant recovery where the two major canopy ecosystems -forests and woodlands - increased considerably in 2006 compared to 1986. These are consistent with the findings of Nicholson (2000); Stow *et al.* (2004) and Lauwaet *et al.* (2009), which suggest that there was a progressive increase in rainfall from late 1980s to the present and a concomitant increase in the vegetation cover of the Sahel belt. However, the transition from woodlands and fallow area to the shrub/grassland category was rapid, which indicates a significant human disturbance.

Under present climate scenario, built-up areas are projected to experience a consistent increase from 1.45% of the area in 2006 to 5.4% in 2046. Area under cultivation is projected to peak at approximately 12% in 2016 (compared to 8% in 2006) and then stabilize around 10% from 2026 to 2046. Unutilized farmland and fallow land is projected to continue to decline with increases in the area under cultivation at any given time and retain only 60% of its 2006 coverage by 2046.

The major canopy ecosystems are very sensitive to changes in climatic parameters, especially rainfall. The overall percent coverage of forest is projected to increase from 15.6% in 2006 to 18% in 2016, and then remain stable at around 15% from 2025 to 2046. The coverage of woodlands is projected to remain above 20% from 2006 to 2046. Some transition from woodlands and fallow lands into forest is also projected. The strongest gain with respect to transitions from one land-cover category to another is projected for the shrub/grassland category, which is expected to increase by approximately 110% over its coverage in 2006, with contributions mainly from woodlands and abandoned farm and fallow lands. Wetlands are projected to consistently decline from approximately 1,650 km<sup>2</sup> in 2006 to less than 600 km<sup>2</sup> in 2046. The area covered by water is also projected to consistently increase, which suggests that water impoundments will likely continue to increase in the near-future. Floodplain agriculture is expected to peak at approximately 7% of the total area in 2016 and then stabilize at approximately 4% from 2026 to 2046.

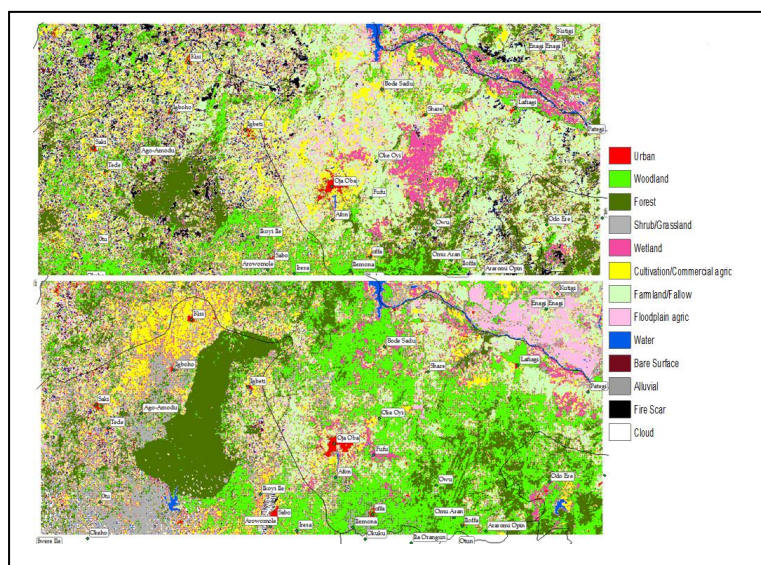


**Fig 5: Landsat image-derived LULC for 1986 (upper) and 2006 (lower)**

The spatial pattern exhibited by the projected LULC changes presents a more interesting scenario. The projected LULC changes for 2016 to 2046 show an increase in the coverage of shrub/grassland in some pocket areas around the northeast, central and southwest axes. These are farmlands and fallow lands transitioning into shrub/grasslands. The protected forest complex is projected to remain

relatively undisturbed, while mosaics of forest and woodland will likely dominate the southeast corridor. From 2006 to 2046, the built-up area is projected to continue to increase. Significantly, the largest growth in built-up land is projected for areas around the northwest to southwest corridor which exhibits strong water footprint in the PCA analysis. In response to increase in built-up area, additional cultivated areas are also projected to emerge around this corridor, which reinforces the strong relationship between agriculture and settlement in rural land use systems.

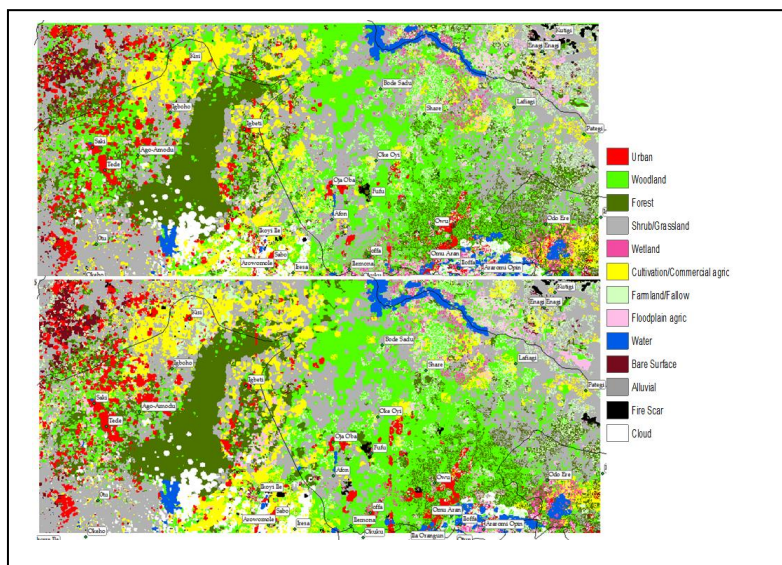


**Fig 6: Projected LULC under the present climate scenario in 2036 (upper), and 2046 (lower)**

#### Projected LULC from the future climate

Future climate scenarios suggest a significant decline in rainfall (approximately 4 mm/month/decade) and an increase (0.02°C/month/decade) in the mean monthly maximum temperature. Table 5 presents a comparison of the projected coverage (in percent) of the LULC categories, and Figure 7 portrays the spatial pattern of the projected LULC under future climate scenarios. Forest is projected to increase from 15.6% in 2006 to approximately 20% in 2016, then decline to about 17% in 2026 and stabilizes at approximately 15% from 2036 to 2046. Compared to the present climate, the projected percentages of forest coverage are expected to be slightly higher under future climate scenarios. Additionally, the

area covered by woodland is expected to progressively increase from 15% in 2016 to 19% by 2046. Again, this increase is slower than under the present climate scenario.

Table 5: Percent coverage of projected LULC for 2006-2046 under future climate scenario

SN	LULC Class	2016	2026	2036	2046
1	Urban	2.84	3.93	4.85	5.36
2	Woodland	15.26	16.57	16.74	19.41
3	Forest	19.91	16.66	15.32	14.66
4	Shrub/grassland	19.33	26.30	26.85	27.16
5	Wetland	2.71	1.61	2.12	1.67
6	Cultivation /commercial agric	7.81	8.54	9.82	10.16
7	Farmland /fallow/grazing area	21.49	16.57	13.20	10.20
8	Floodplain agric	3.86	3.24	3.69	3.60
9	Water	1.21	1.64	2.07	2.42
10	Bare surface	1.07	1.32	1.54	1.59
11	Alluvial	0.02	0.01	0.01	0.01
12	Burnt surface	0.74	0.49	0.53	0.52
13	Cloud /shadow	3.74	3.13	3.27	3.22

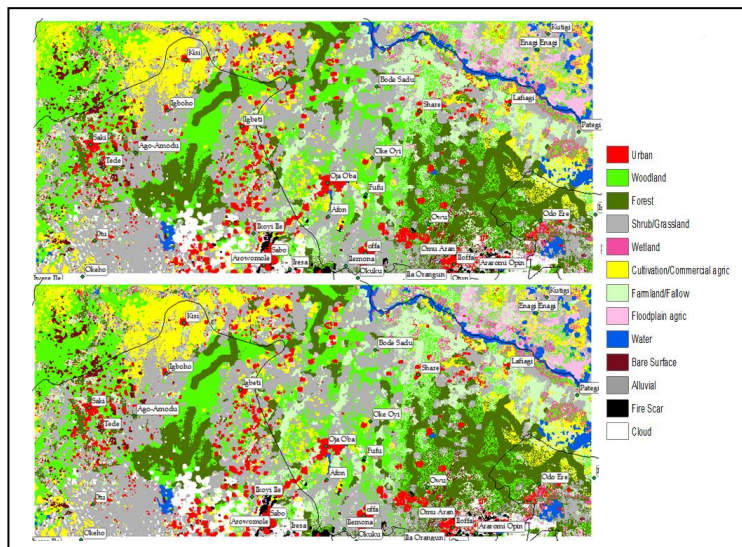


Fig 7: Projected LULC under future climate scenarios in 2036 (upper) and 2046 (lower)

Moreover, the major difference between the simulated LULC pattern under the present and future climate scenarios is clear from the spatial pattern of the simulated LULC categories. Under the future climate scenario, the forests would likely become more disturbed, with galleria forest becoming the most significant forest type, and shrub and grassland will also become much more widespread. Galleria forest and widespread shrub/grassland generally typify the drier parts of the Savannah. This suggests that under the future climate scenario, the wooded savannah will likely become drier, and the

vegetation pattern may change dramatically. This is consistent with the reduction in the water footprint expected under future climate scenario. The spatial pattern of urban lands suggests that more settlements are projected to emerge around the middle region, mainly along the Oyo, Ogbomosho, Igbeti and Ilorin axis, compared to the western axis under present climatic conditions. This is also consistent with the expected decline in the spatial influence of the climate-orographic complex that controls the local climate that will weaken the local system on the western axis and reduce the water footprint under the future climate scenario. This could partly explain why the expansion of existing settlements and the emergence of new built-up areas may favour the middle region, especially at the edge of the protected areas, where wetter conditions are projected to dominate under the future climate.

### **Model validation and calibration**

With the 1986 and 2000 maps representing the basis land-cover, a map for 2006 was simulated using a 6-month time-step. The kappa index between the simulated and true maps for 2006 was computed. The areal agreements between the real and simulated maps and their spatial patterns were compared. The agreement in terms of quantity was good and was almost equal for most of the categories. The essential features of the area, including the large track of protected area, cultivated lands around the northwest, water impoundments, river networks, shrub/grasslands around the south-west, the floodplain of the Niger River, and the mosaic of forests and woodlands around the southeast were captured well. The greatest uncertainty is the confusion between the woodland areas on the real map and the shrub/grassland areas on the simulated map which led to very poor kappa index of 0.45. A lack of field confirmation and accuracy assessments of the image-derived land-cover maps may have contributed to this poor agreement. Another possible explanation for this is the lack of an intermediate map (for the 1990s). Hence, the model might have difficulty capturing the abrupt transition from the drought years of the 1980s to the relatively wet years of the 2000s.

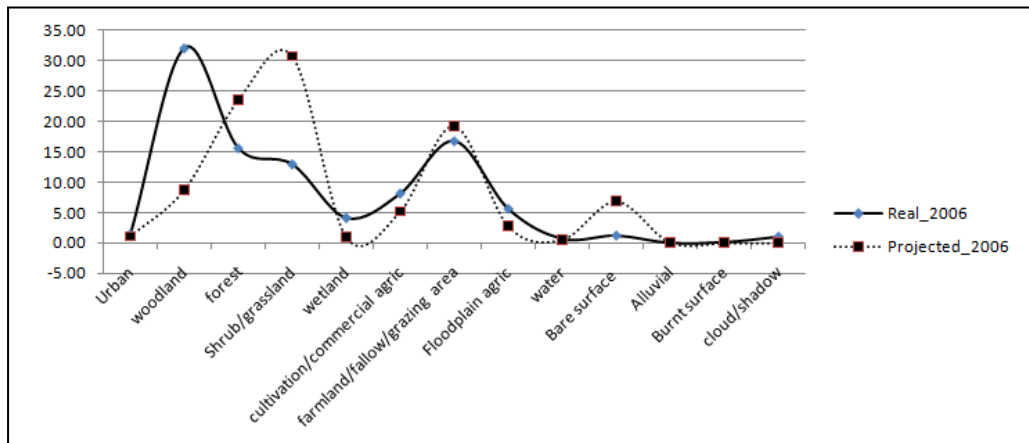


Fig 7: Coverage (in percent) of LULC categories for real and simulated maps for 2006

The simulation results are projections based on the assumed climatic scenarios; they represent a quantified visualization of qualitative scenario descriptions. Uncertainty notwithstanding, they are important as guide for decisions related to land management, nature and biodiversity conservation, forest management and ecotourism, which are critical for climate change mitigation and adaptation.

## Conclusions

The main issue addressed in this study is that water footprint has the potential to influence the patterns of land systems changes across space and time in complex and heterogeneous agrarian landscape. Under both present and future climate scenarios, built-up areas are projected to experience a consistent increase. Rural to rural migration in search of favourable agricultural land is expected to be significant, but the resulting spatial pattern is projected to substantially follow the water footprints created by the local climate. This may also present a potential for increased resource-induced conflicts. There is also the possibility of dramatic changes in vegetation patterns as the wooded savannah becomes drier with galleria forest becoming the dominant forest type. Therefore, measures to protect current forests and woodlands are critical for sustaining present climate-ecology relations and current water footprint.

## Acknowledgments

This research was carried out under the African Climate Change Fellowship Programme (ACCFP). The ACCFP is supported by a grant from the Climate Change Adaptation in Africa (CCAA), funded

jointly by the International Development Research Centre (IDRC) of Canada and the UK's Department for International Development (DFID). The International START Secretariat is the implementing agency, in collaboration with the Institute of Resource Assessment (IRA) of the University of Dar es Salaam and the African Academic of Sciences (AAS).

## References

- Abiodun, B.J., Pal, J.S., Afiesimama, E.A., Gutowski, W.J., and Adedoyin, A. (2008), "Simulation of West African monsoon using RegCM3 Part II: impacts of deforestation and desertification", *Theoretical and Applied Climatology*, 93, 245-261.
- Adisa, S.R., and Adekunle, O.A. (2010), "Farmer-Herdsmen Conflicts: A Factor Analysis of Socio-economic Conflict Variables among Arable Crop Farmers in North Central Nigeria" *Journal of Human Ecology*, 30 (1), 1-9.
- Afiesimama, E.A., Pal, J.S., Abiodun, B.J., Gutowski Jr, W.J., and Adedoyin, A. (2006), "Simulation of West African monsoon using the RegCM3.Part I: Model validation and interannual variability", *Theoretical and Applied Climatology*, 86, 23-37
- Akinbami, J.F.K., Salami, A.T., & Siyanbola, W.O. (2003). An integrated strategy for sustainable forest-energy-environment interactions in Nigeria. *Journal of Environmental Management* 69, 115-128. doi:10.1016/S0301-4797(03)00083-5
- Anderson, J.R., Hardy, E.E., Roach, J.T., Witmer, R.E. (1976), "A Land use and Land cover Classification System for use with Remote Sensor Data" *Geological Survey Professional Paper* 964
- Bucini, G., and Lambin, E.F. (2002), "Fire impacts on vegetation in Central Africa: a remote-sensing-based statistical analysis" *Applied Geography*, 22 (2002), 27-48.
- Cook, K.H., and Vizy, E.K. (2006), "Coupled Model simulation of the West African Monsoon Systems: Twentieth- and Twenty-First Century Simulations", *Journal of Climate*, 19, 3681-3703.
- Eastman, J.R. (2009), *Idrisi Taiga Guide to Image Processing*, USA: Clark Labs, Worcester, MA.
- Fasona, M., Omojola, A., Adeaga, O., and Dabi, D. (2007), "Aspects of Climate Change and Resource Conflicts in the Nigeria Savannah". *IPCC/TGICA Expert Meeting on Integrating Analysis of Regional Climate Change and Response Options*, Nadi, Fiji Islands, Available Online, [http://www.ipcc.ch/pdf/supporting-material/tgica\\_reg-meet-fiji-2007.pdf](http://www.ipcc.ch/pdf/supporting-material/tgica_reg-meet-fiji-2007.pdf)
- Fasona, M.J., and Omojola, A.S. (2005), "Climate Change, Human Security and Communal Clashes in Nigeria", *Proceedings of International Workshop on Human Security and Climate Change*, 22-23 June 2005, Asker, Oslo, Available online, [www.gechs.org/activities/holmen/Fasona\\_Omojola.pdf](http://www.gechs.org/activities/holmen/Fasona_Omojola.pdf).
- German Advisory Council on Climate Change (2008), *Climate Change as a security risk*, U.K: Earthscan
- Hall, C.A.S., Tian, H., Qi, Y., Pontius, G., and Cornell, J. (1995), "Modelling Spatial and Temporal Patterns of Tropical Land Use Change", *Terrestrial Ecosystem Interactions with Global Change*, 2, 753-757.
- Hewitson, B.C., and Crane, R.G. (2006), "Consensus between GCM climate change projections with empirical downscaling: precipitation downscaling over South Africa", *International Journal of Climatology*, 26, 1315-1337
- Hoffmann, W.A., and Jackson, R.B. (2000), "Vegetation-Climate Feedbacks in the Conversion of Tropical Savannah to Grassland", *Journal of Climate*, 13, 1593-1602

- Kottek, M., Grieser, J., Beck, C., Rudolf, B., Ru, F. (2006), "World map of the Köppen-Geiger climate classification updated", *Meteorologische Zeitschrift*, 15(3), 259-263.
- Lauwaet, D., van Lipzig, N.P.M., and De Ridder, E.K. (2009), "The effect of vegetation changes on precipitation and Mesoscale Convective Systems in the Sahel" *Dynamic Climatology*, 33, 521-534
- MacKellar, N.C., Tadross, M.A., and Hewitson, B.C. (2009), "Effects of vegetation map change in MM5 simulations of southern Africa's summer climate", *International Journal of Climatology*, 29, 885-898
- Nicholson, S. (2000), "Land surface processes and Sahel climate", *Reviews of Geophysics*, 38(1), 117-339.
- Obioha, E.E. (2008), "Climate Change, Population Drift and Violent Conflict over Land Resources in North-eastern Nigeria", *Journal of Human Ecology*, 23(4), 311-324.
- Odekunle, T.O., Balogun, E. E., and Ogunkoya, O.O. (2005), "On the prediction of rainfall onset and retreat dates in Nigeria", *Theoretical and Applied Climatology*, 81, 101-112
- Omotosho, J.B., and Abiodun, J. (2007), "A numerical study of moisture build-up and rainfall over West Africa". *Meteorological Applications*, 14, 209-225.
- Pielke Sr. R.A., Adegoke, J., Beltran-Przekurat, A., Hiemstra, C.A., Lin, J., Nair, U.S., Niyogi, D., and Nobis, E. (2007), "An overview of regional land-use and land-cover impacts on rainfall", *Tellus* 59B (3), 587-601.
- Pontius Jr, G.R., and Malanson, J. (2005), "Comparison of the structure and accuracy of two land change models", *International Journal of Geographical Information Science*, 19(2), 243- 265.
- Pontius Jr, R.G., and Schneider, L.C. (2001), "Land-cover change model validation by an ROC method for the Ipswich watershed, Massachusetts, USA", *Agriculture, Ecosystems and Environment*, 85, 239-248.
- Solomon, S., Qin, D., Manning, M., Alley, R.B., Berntsen, T., Bindoff, N.L., Chen, Z., Chidthaisong, A., Gregory, J.M., Hegerl, G.C., Heimann, M., Hewitson, B., Hoskins, B.J., Joos, F., Jouzel, J., Kattsov, V., Lohmann, U., Matsuno, T., Molina, M., Nicholls, N., Overpeck, J., Raga, G., Ramaswamy, V., Ren, J., Rusticucci, M., Somerville, R., Stocker, T.F., Whetton, P., Wood, R.A., Wratt, D. (2007), Technical Summary, *The Physical Science Basis. Contribution of Working Group I to the Fourth Assessment Report of the Intergovernmental Panel on Climate Change, Climate Change 2007* eds. S.Solomon., D. Quin., M. Manning., Z.Chen., M. Marquis., K.B. Averyt., M. Tignor., and H.L. Miller, Cambridge, UK: Cambridge University Press.
- Stow, D.A., Hope, A., McGuire, D., Verbyla, D., Gamon, J., Huemmrich, F., Houston, S., Racine, C., Sturm, M., Tape, K., Hinzman L., (Professor of Water Resources), Yoshikawa, K., Tweedie, C., Noyle, B., Silapaswan, C., Douglas, D., Griffith, B., Jia, G., Epstein, H., Walker, D., Daeschner, S., Petersen, A., Zhou, L., and Myneni, R. (2004), "Remote sensing of vegetation and land-cover change in Arctic Tundra Ecosystems", *Remote Sensing of Environment*, 89, 281-308.
- Taylor, C.M., Lambin, E.F., Stephenne, N., Harding, R.J., and Essery, R.L. (2002), "The Influence of Land Use Change on Climate in the Sahel", *Journal of Climate*, 15, 3615-3629.
- Tiwari, R., Murthy, I.K., Killi, J., Kandula, K., Bhat, B.R., Nagarajan, R., Kommu, V., Rao, K.K., and Ravindranath, N.H. (2010), "Land use dynamics in select village ecosystems of southern India: drivers and implications", *Journal of Land Use Science*, 5, (3), 197-215.
- Verburg, P.H., Eickhout, B., and Meij, H. (2007), "A multi-scale, multi-model approach for analyzing the future dynamics of European land use", *Annals of Regional Science*, doi 10.1007/s00168-007-0136-4.
- Wang, G. L., and Eltahir, E. A. B. (2000), "Biosphere-atmosphere interactions over West Africa. II: Multiple climate equilibria", *Quarterly Journal of Royal Meteorological Society*, 126, 1261-1280
- Weng, Q. (2002), "Land use change analysis in the Zhujiang Delta of China using Satellite remote sensing, GIS and stochastic modelling", *Journal of Environmental Management*, 64, 273-284.